Accepted Manuscript

Experimental studies of explosion energy output with different igniter mass

Heyang Xu, Weibing Li, Wenbin Li, Yajun Wang

PII: S2214-9147(19)30204-1

DOI: https://doi.org/10.1016/j.dt.2019.05.010

Reference: DT 451

To appear in: *Defence Technology*

Received Date: 28 February 2019

Revised Date: 25 April 2019

Accepted Date: 20 May 2019

Please cite this article as: Xu H, Li W, Li W, Wang Y, Experimental studies of explosion energy output with different igniter mass, *Defence Technology* (2019), doi: https://doi.org/10.1016/j.dt.2019.05.010.

EXPERIMENTAL STUDIES OF EXPLOSION ENERGY OUTPUT WITH DIFFERENT IGNITER MASS

Abstract: For study the energy output law of cylindrical charge with shell induced by different input energies, four different black powder masses were selected to ignite the main charge. Fragmentation degree of the shell was qualitatively analyzed by the area of holes on the witness plate and the recovered fragment mass. Through theoretical analysis, established the functional relationship between the average mass of fragments and the relative energy output of warhead, obtained how the relative energy output of charge changed with different initial energy input. The results showed that the change of input energy could lead to obvious variation in fragment characteristics, and could also control the output of charge. When the igniter mass increases from 1.55 g to 5.00 g, the relative energy output of the charge increases by 26.28%. Excessive initial input energy will destroy the shell confine in advance, resulting in a decrease in the relative energy output of charge

1. Introduction

An increasing number of asymmetric conflicts, often within urban terrains, require the warhead not only to destroy established targets effectively but also to bring as little incidental risk as possible. But today's warheads are generally designed to maximize their damage effectiveness, while providing a full-output mode only. Therefore, more and more researchers begin to pay attention to the adjustability of damage effect[1−2].

There are two main control methods to adjust the energy release. One is the compound charge, which combines two kinds of high explosives with different detonation performance, separated by flameproof materials. Depending upon this principle, the British company QinetiQ[3−4] proposed a multi-layer ring nested compound charge structure composed of high explosive, aluminum-containing explosive and flameproof materials, and successfully realized two-stage power output of cased charge. Peter Haskins[5] and Hong X W et al.[6−7] also studied similar structures. However, the charge structure of this method is quite complex, and the energy output level is relatively fixed, generally just 2−3 grades. Another method to control the multi-stage output of energy is controlling the reaction intensity of the single high explosive. Compared with the multi-layer compound charge, the structure to control the reaction intensity of explosive is simpler, meanwhile more output grades can be implemented. Besides the physical and chemical properties of the explosive [8−9] and filling density[10], the initial input energy[11], external constraints[12] and ambient temperature[13] also affect the reaction intensity of explosives. For warheads, input energy gets a better choice, because it is more controllable than constraint and ambient temperature. Bernecker.R.R.et al.[11] believed that weaker igniters would delay the reaction process of low-density particulate beds and lead to lag of compression combustion (hot spot). Later, RONG Guangfu et al.[14] further verified that the probability of initiating pressed high-density charging by high-energy igniter was higher than by low-energy igniter. However, they only compared two kinds of input energies but did not do more studies. CHEN Wei et al.[15] made a systematic study on the process of deflagration to detonation transition while loading different igniter mass. It was found that when the igniter mass was between 0.20 g~5.00 g, the output energy would increase with the increase of igniter mass. But it was just a qualitative result

from fragments and indentation on steel plates. Arnold W.[16] also proposed a new type of warhead at the International Ballistic Conference, claimed that 0 % to 100 % of the charge energy output can be achieved through the cooperation of different detonation modes. Subsequently, Graswald M. et al. [17] carried out further experimental studies on the basis of Arnold, and confirmed that the warhead could achieve multi-range output of energy through the holes on the witness plate and partially recovered fragments. However, most of the above studies only analyzed the output energy based on fragment size, witness plate, indentation qualitatively, while few could describe the output energy of warhead quantitatively.

In this paper, we were studied on the output energy of RDX-based pressed explosive ignited by different igniter mass. The number and area of holes on the witness plates and the recovered fragments with different input energy were analyzed. Established the calculation formula between the average mass of fragments and the relative energy output of warhead, and then the relative energy output of warhead with different input energy was calculated

2. Experiments design

Black powders with four different mass were used to detonate the main charge. The test sample is a hollow cylindrical steel tube with a diameter of 61.5 mm and a wall thickness of 15mm. Both ends were bound with an end cap. The total length of the tube is 290mm. The RDX-based pressed explosive with a density of 1.69 g/cm^3 and a detonation velocity of 8 425 m/s is filled in the steel tube. There was a fixed room above main charge and filled with 1.55 g, 3.07 g, 5.00 g, and 10.07 g black powders respectively (other conditions being equal), which are used to generate four different amounts of input energy. The size of black powder used in this test is about 0.71~1.25 mm, the loading density is 1.1 g/cm^3, and the heat of detonation is 2 450 kJ. The Gurney constant of explosive $\sqrt{2E} = 2\,801$ m/s

Fig. 1 shows the layout of the test and the details of the sample. Spectrophotometry was used to ignite the black powder at the top of charge in the test. Aluminum plates with a thickness of 2 mm were used as a witness plates, which were placed at a horizontal distance of 1.5 m from the charge, the size of the witness board is 1.5 m×1.0 m. The center of the charge is 75 mm high to ensure that the geometric center of the witness plate is at the same vertical height. The Experiments was completed in a sealed explosion castle so that we could recover fragments as completely as possible after tests. And we used recovered fragments and holes on the witness plates to reflect the relative energy output of the main charge.

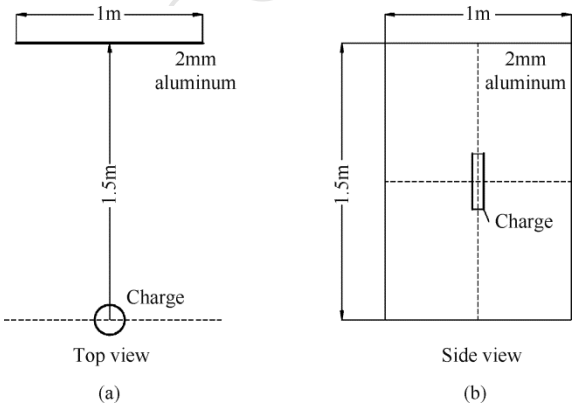

Fig. 1 Sketch of warhead initiation by black powder and components' photo (a) and test setup with 2mm Aluminum witness plate (b)

3. Experimental results and analysis

3.1 Result of witness plates

The left side of Fig. 2 shows the witness plates after the test. The profile and area of the holes on the aluminum plates are positively correlated with the profile and area of the fragments' windward surface, which can reflect fragmentation of the shell[18]. However, the holes on the witness plates are irregular polygons, so it is impossible to get the effective information on the witness plates directly, if the perforation images are not processed. Photographs were taken under strong illumination, which could make the contrast of the holes easily distinguished from other areas. After binarization, holes information can be easily obtained by using computer vision detection technology and multi-level gray subdivision technology. Hole boundaries were stored as closed polygons, from which data such as central location, area, and size can be calculated.

Fig. 2 presents intuitive processed images on the right side. It is clearly seen that the position of fragments bands is basically similar and below the midline in four conditions. The number of holes in case 1 and case 4 is obviously smaller than that in other two cases, and the holes area in case 4 is bigger than that in others.

Case 1 1.55g black powder

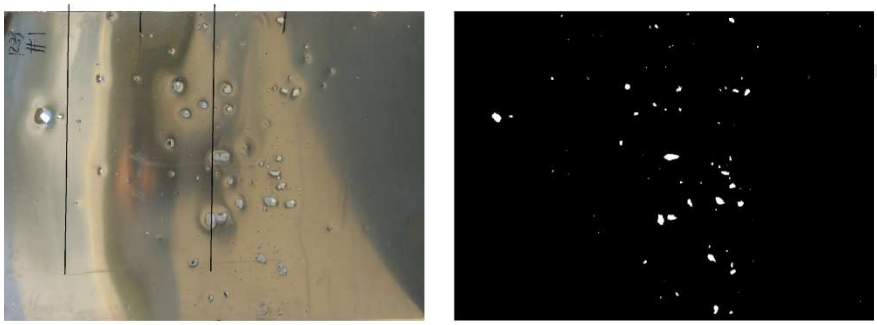

Case 2 3.07g black powder

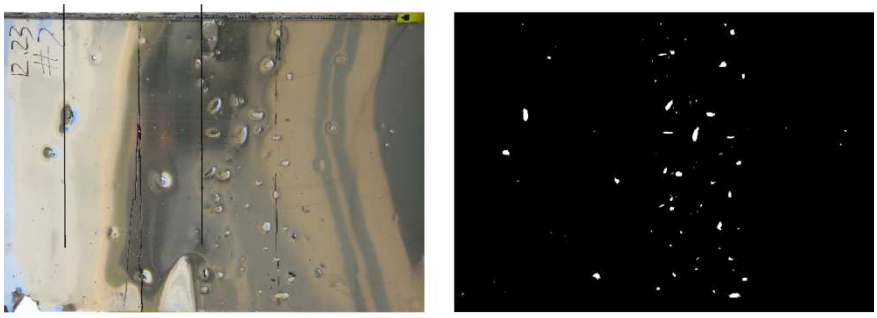

Case 3 5.00g black powder

Case 4 10.07g black powder

Fig. 2 Witness plates after test which left side are top (left) and the processed image for evaluation (right)

Fig. 3 presents the counted results of the holes' area and cumulative number of holes in four conditions, in which holes' area is sorted by increasing order. The number of holes in case 2 and case 3 is close, 78 and 79, respectively, far greater than that in case 1 and case 4, which is 46 and 48 respectively. From large to small order, the average area of holes is $\bar{A}_{c4} > \bar{A}_{c1} > \bar{A}_{c2} > \bar{A}_{c3}$. The results of case 2 and case 3 are similar in the number and average area of holes, but there are obvious differences compared with case 1 and case 4. This proves that energy output varies with the input energy, and the igniter could be used to control the energy output of warhead.

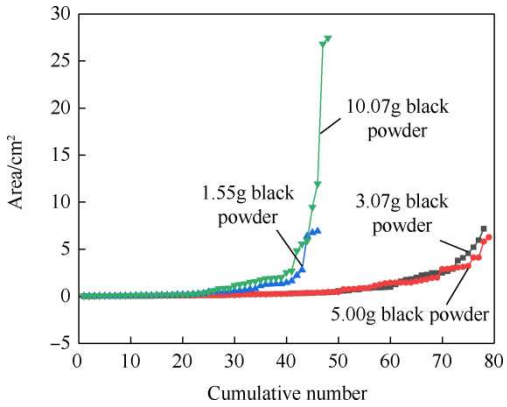

Fig. 3 An ascending sort of the holes' area from witness plates for every case

3.2 Average mass of fragments

Only one witness plate was set up in the experiment to reduce the secondary breakup of fragments. The witness plate covers a scattering angle of 37° and does not fully reflect the overall characteristics. In order to reflect fragmentation accurately, the fragments were completely recovered in this test, rather than a simpler partial recovery.

Fig. 4 shows recovered fragments from the warhead initiated by1.55 g, 3.07 g, 5.00 g, and 10.07 g black powders. Different from detonator initiation, the size and mass of the fragments recovered from ignited warhead vary over a large scale. The mass ranges from a few grams to several hundred grams and the size from millimeters to hundreds of millimeters. This is due to the whole process involving complex physical and chemical changes, the time and space are needed to support the transition from combustion to detonation when it was ignited. In the early stage, the low-speed combustion becomes the accelerating compaction wave. There is an induction time after the compaction wave passes over material until any reactions and gas generation become significant. Therefore, the strain rate of the shell is at a relatively low level, which leads the shell to tearing along the axis, so that fragments have a long strip and large size. The wave grows in strength as the pressure in the burning region increases and until it is sufficiently strong to initiate the explosive. At this stage, the shell is divided into smaller fragments.

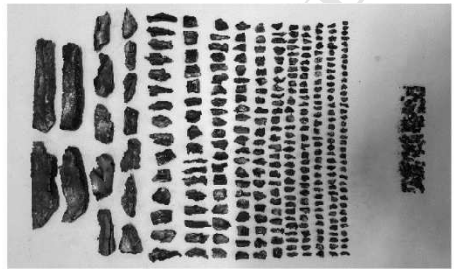

Case 1

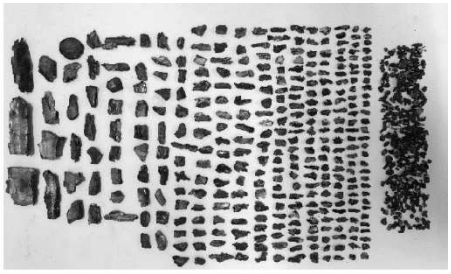

Case 2

Case 3

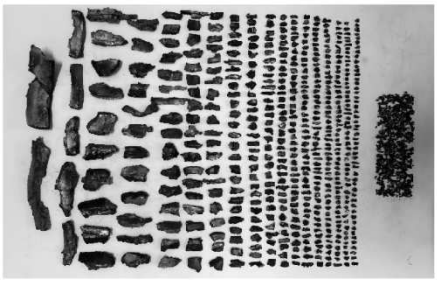

Case 4

Fig. 4 The recovered fragments of shell ignited by 1.55 g, 3.07 g, 5.00 g, and 10.07 g black powder respectively

All fragments were weighed and counted, and their average mass was calculated. The results are shown in Fig. 5. Compared with case 1 and case 4, case 2 and case 3 have more fragments and smaller fragmentation quality. When the mass of black powder increases from 1.55 g to 5.00 g, the average mass of fragments decreases from 7.47 g to 3.97 g, a decrease of 46.9%, and the number of small fragments increases gradually. When the mass of black powder increased to 10.07 g, the average mass of fragments increased again to 6.18g. Ignited by four input energies, there is a slight difference in the degree of shell fracture reflected by the average area of holes and the average mass of fragments (the average area of holes is $\bar{A}_{c4} > \bar{A}_{c1}$, but the average mass of fragments is $\bar{m}_{c1} > \bar{m}_{c4}$). We believe that the result of recovered fragments is correct, because there were larger error comes from little witness plates.

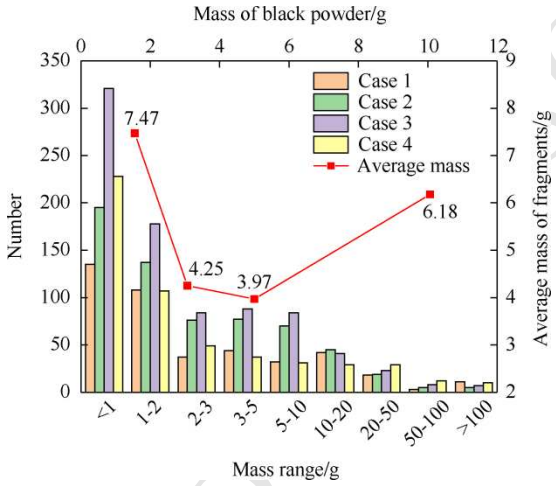

Fig. 5 Number of fragments in different ranges (Histogram) and the average mass of fragments (Line) ignited by 3.07 g, 5.00 g, 1.55 g, and 10.07 g black powder

3.3 Relative energy output

The shell withstands high strain rates under blast loading, and higher strain rate will result in a larger circumferential splitting number, means smaller fragments. Therefore, it is more convenient to use the mass of fragments to infer output energy when the energy is difficult to measure, such as incomplete detonation.

For uncontrolled fragment warhead, Mott and Linfoot[19] proposed that under explosion conditions, when a crack is formed instantaneously during shell rupture, the per unit area of per thickness required energy *W* can be approximately expressed as follows:

$$W = \frac{1}{24}\rho_0 v_0^2 \frac{l_2^3}{a_f^2} \tag{1}$$

Where, ρ_0 is the density of shell (g/cm^3), l_2 is the distance between cracks (cm), a_f is the radius of the instantaneous rupture of the shell (cm), v_0 is the expansion velocity of the instantaneous rupture of the shell (m/s), and the value of *W* can be determined by collision test or theoretical calculation[20].

Mott pointed out in subsequent research reports that the ratio of length l_1 to width l_2 of fragments satisfies certain statistical rules. If the ratio is β, the length can be expressed as $l_1 = \beta l_2$. For steel, the ratio is roughly $l_1 : l_2 = 3.5 : 1$. The fragments size shown in Fig. 4, did not

like full detonation, have an obvious transformation, and the ratio may not apply. So that all recovered fragments in four cases were measured and counted by image software, and the statistical results were shown in Fig. 6. The aspect ratio distribution exhibited a step-like nature shown in Fig. 6, which means that the aspect ratio may be quantized. The means of aspect ratio are 1.98, 1.96, 1.99 and 1.97, and the median of aspect ratio are1.83, 1.84, 1.87 and 1.79. For bell-shaped distribution, median could exclude the effect of extremes, and reflect the overall level more accurately, therefor the median was used to calculated.

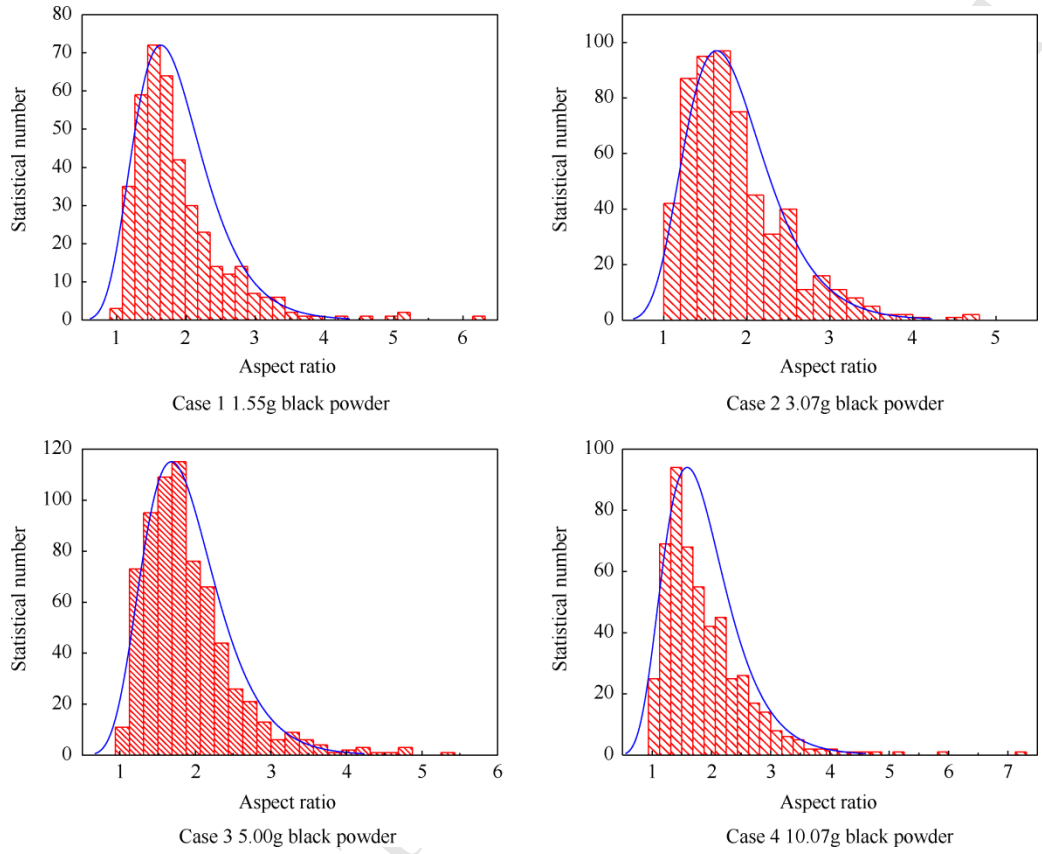

Fig. 6 Statistical results of aspect ratio of received fragments ignited by 3.07 g, 5.00 g, 1.55 g, and 10.07 g black powder

If the thickness of the fragment is δ, the average mass of the fragment can be expressed as:

$$\overline{m}_{\mathrm{f}} = l_1 l_2 \delta \rho_0 = \beta l_2^2 \delta \rho_0 \tag{2}$$

Simultaneous Eq. (1) and Eq. (2) available:

$$\overline{m}_{\mathrm{f}} = 8.32 \frac{\beta \rho_0^{1/3} a_{\mathrm{f}}^{4/3} W^{2/3} \delta}{v_0^{4/3}} \tag{3}$$

Assume that the initial state quantities of the shell before expansion are a_0 and δ_0 respectively, and ε satisfies $a_{\mathrm{f}} = \varepsilon a_0$, so that δ can be obtained according to the volume of shell is constant, that is

$$(a_{\mathrm{f}} + \delta)^{\gamma+1} - a_{\mathrm{f}}^{\gamma+1} = (a_0 + \delta_0)^{\gamma+1} - a_0^{\gamma+1}$$

Ignore high-order small quantities of δ and δ_0, for cylindrical shell $\delta = \delta_0/\varepsilon$, ε is determined by material properties. In this paper, we take $\varepsilon = 1.67$[21]。

According to Gurney's research, fragment velocity can be expressed as

$$v_0 = \sqrt{2E}\left(\frac{M}{C} + \frac{1}{2}\right)^{-1/2} \tag{4}$$

Substituting the Eq. (4) into the Eq. (3), so that we can establish the relationship between the average mass of fragments and charge quality as

$$\left(\frac{8.32\beta\rho_0^{1/3}a_{\mathrm{f}}^{4/3}W^{2/3}\delta}{\overline{m}_{\mathrm{f}}}\right)^{3/4}=\sqrt{2E}\left(\frac{M}{C}+\frac{1}{2}\right)^{-1/2}$$

simplify as

$$\frac{M}{C}=\left(\sqrt{2E}\right)^2\left(\frac{\Psi}{\overline{m}_{\mathrm{f}}}\right)^{-3/2}-\frac{1}{2}$$

Where $\Psi=8.32\beta\rho_0^{1/3}a_{\mathrm{f}}^{4/3}W^{2/3}\delta$, $\sqrt{2E}$ is Gurney constant, C is the charge mass and M is the shell mass.

For warheads with large wall thickness, the revised fragment velocity formula[22] is $v_0=\sqrt{2E}\sqrt{(C/M)/\left\{\left(1+\frac{C}{2M}\right)\left(1+\frac{D_{\mathrm{e}}}{2L}\right)\right\}}$, the corresponding functional relationship can be obtained

$$\frac{M}{C}=\frac{\left(\sqrt{2E}\right)^2}{\left(\frac{\Psi}{\overline{m}_{\mathrm{f}}}\right)^{3/2}\left(1+\frac{D_{\mathrm{e}}}{2L}\right)}-\frac{1}{2}$$

Where, D_{e} is charge diameter and L is shell length. Therefore, when the structure and material of warhead have been determined, we can use the above equation to calculate the effective charge mass through average mass of fragments.

Fragmentation of 40CrMnSiB was studied in reference [21]. The process of shell expansion fracture, fragment mass distribution and fragment fracture characteristics were described comprehensively in this paper. Therefore, we use it to verify the above formula. In this reference, the average mass of fragments is 0.345 g. The corresponding charge mass can be calculated to be 297.120 g by using the formula above, while the actual charge mass is 304.730 g. The error is just 2.6%, which proved the formula can accurately describe the relationship between the average mass of fragments and the effective charge quality.

The effective charge mass with different input energies was calculated by using the average mass of fragments obtained in the test. If the energy from the complete detonation of charge is defined as 1, the relative energy output of warhead with different input energies can be obtained, as showed in Fig. 7.

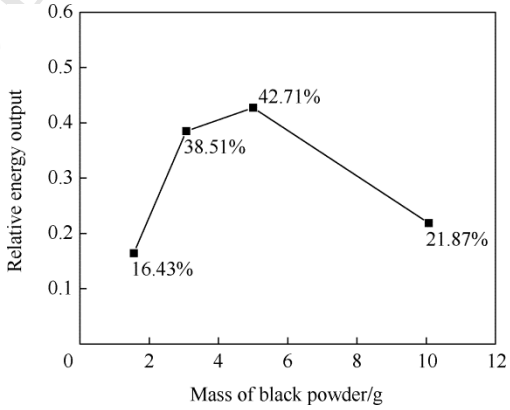

Fig. 7 relationship between the mass of black powder and relative energy output which calculated from the average mass of fragments

From Fig. 7, it can be clearly seen that the relative energy output increases first and then decreases with the increase of the mass of black powder. When the mass of black powder increases from 1.55 g to 5.00 g, the relative energy output of the charge increases continuously, from 16.43% to 42.71%. Because the increase of the initial input energy is beneficial to the accumulation of energy, thereby accelerates the reaction rate of the charge. When the black powder is increased to 10.00 g, the relative energy output does not increase as expected, but decreases to only 21.87%. There will be a sudden increase in pressure, when a large number of igniters are ignited. High pressure will directly destroy the shell confinement, resulting in a rapid drop of pressure in the tube. The propagation of sparse waves reduces the pressure in the explosive and delay the transition time of the combustion to the detonation.

4. Conclusion

In this paper, the energy output of warhead with different input energies was studied. 1.55 g, 3.07 g, 5.00 g, and 10.07 g black powders were used to ignite cylindrical shell filled with RDX-based pressed charge. Through the characteristics of holes on the witness plates and the quality of recovered fragments, it can be seen that different input energies have an obvious influence on the fragmentation of shell. The functional relationship between the average mass of fragments and the relative energy release of charge was established, and then the law of relative energy output of cylindrical charge and initial input energy was obtained. When the igniter quantity increases from 1.55 g to 5.00 g, the relative energy output of the charge increases by 26.28%. While excessive initial input energy will prematurely destroy the shell confinement, resulting in a decrease in the relative energy output of the charge.

Acknowledgments

The work presented in this paper has been funded by the National Natural Science Foundation of China No. 11202103 and Jiangsu Province Innovation Program No. KYCX18_0472.

References

[1] Zang Xiaojing, Jiang Qi, Adjustable power of conventional warhead[J]. Winged Missiles Journal, 2011(4): 90-91, 97.

[2] Arnold W. Rottenkolber E. Axially Switchable Modes Warheads[C]// 28th International Symposium on Ballistics, Atlanta, GA, USA, 2014, 289-300

[3] Colclough M E. A novel tuneable effects explosive charge[C]//NDIA IM&EM Symposium. Las Vegas, NV: Nation Defense Industrial Association,2012.

[4] Reynolds M, Huntington-Thresher W. Development of tuneable effects warheads[J]. Defense Technology, 2016, 12(3): 255-262.

[5] Haskins P. Controllable output warhead[P], EP2564150A1, 2011.

[6] HONG Xiao-wen, LI Wei-bing, CHENG Wei, et al. Failure Process and Dynamic Response of Masonry Wall under Blast Loading of Composite Charge[J].,2018,41(5):471-478.

[7] Hong X W, Li W B, Wang X M, et al. Explosion Temperature and Dispersion Characteristics of Composite Charges Based on Different Non-detonative Materials[J]. Propellants, Explosives, Pyrotechnics, 2018.

[8] QIN Neng, LIAO Lin-quan, JIN Peng-gang, et al. Experimental study on deflagration-to-detonation transition of solid propellants [J]. Chinese Journal of Explosives & Propellants, 2010, 33(4): 86-89.

[9] Charles E H. An insensitive nitrocellulose base high performance minimum smoke propellant[C]//Proceeding of Insensitive Munitions Technology Symposium, ADPA, Williamsburg, VA. 1994: 221-228.

[10] JIA Xiang-rui, LI Dong-xiang, SUN Jin-shan, et al. An analysis of the deflagration-to-detonation transition (DDT) in NEPE propellants[J]. Acta Armamentarii, 1997, 18(1): 46-51.

[11] Bernecker R R , Price D , Sandusky H . Burning to Detonation Transition in Porous Beds of a High Energy Propellant[J]. Combustion and Flame, 1979, 48(3):77.

[12] Lang C, Fei W, Jun-Ying W, et al. Investigation of the Deflagration to Detonation Transition in Pressed High Density Explosives[J]. Chinese Journal of Energetic Materials, 2011.

[13] Xiao‐Gan Dai, Yu‐Shi Wen, Feng‐Lei Huang, et al. Effect of Temperature, Density and Confinement on Deflagration to Detonation Transition of an HMX-Based Explosive[J]. Propellants Explosives Pyrotechnics, 2014, 39(4):563-567.

[14] RONG Guang-fu，HUANG Yin-sheng. Influence of Two High-energy Ignition Compositions on Transformation of Combustion to Detonation of Explosives[J]. Explosive Materials, 2008, 37(5): 20-22 .

[15] CHEN Wei, ZHENG Yu, WANG Xiaoming, et al. Experimental Research on the Effect of Ignition Composition Quantity on the Explosion Energy Generation[J]. Explosive Materials, 2013(4):10-13.

[16] W. Arnold, Tunable Charge[C]//20th International Symposium on Ballistics, Orlando, Florida, USA, 2002.

[17] Graswald M, Arnold W. Experimental studies of scalable effects warhead technologies[C]// 26th International Symposium on Ballistics. Miami, Florida, USA. 2011, 201(1).

[18] Arnold W, Rottenkolber E. Fragment mass distribution of metal cased explosive charges[J]. International Journal of Impact Engineering, 2008, 35(12):1393-1398.

[19] Mott, N. F. Fragmentation of Shell Cases [J]. Proceedings of Royal Soc., 1947, 189, p300-308.

[20] Lloyd R. Conventional warhead systems physics and engineering design[M]. American Institute of Aeronautics and Astronautics, Inc. 1998.

[21] Zhu Jian-jun, Li Wei-bing, Li Wen-bin, et al. Dynamic Deformation and Fracture Fragmentation behavior of Metal Cylindrical Shell at High Strain Rates[J]. Acta Armamentarii, 2017, 38(10):1933-1941.

[22] Lloyd R. Overview of Kinetic Energy Rod Warhead Technology[C]// Multinational Conference on Theater Missile Defense, Munich, Germany, 1996